Quantum Error Correction in Scrambling Dynamics and Measurement-Induced Phase Transition

Soonwon Choi,[1] Yimu Bao,[1] Xiao-Liang Qi,[2] and Ehud Altman[1,3]
[1]Department of Physics, University of California Berkeley, Berkeley, California 94720, USA
[2]Stanford Institute for Theoretical Physics, Stanford University, Stanford, California 94305, USA
[3]Materials Science Division, Lawrence Berkeley National Laboratory, Berkeley, California 94720, USA

(Received 31 March 2019; accepted 12 June 2020; published 15 July 2020)

We analyze the dynamics of entanglement entropy in a generic quantum many-body open system from the perspective of quantum information and error corrections. We introduce a random unitary circuit model with intermittent projective measurements, in which the degree of information scrambling by the unitary and the rate of projective measurements are independently controlled. This model displays two stable phases, characterized by the volume-law and area-law scaling entanglement entropy in steady states. The transition between the two phases is understood from the point of view of quantum error correction: the chaotic unitary evolution protects quantum information from projective measurements that act as errors. A phase transition occurs when the rate of errors exceeds a threshold that depends on the degree of information scrambling. We confirm these results using numerical simulations and obtain the phase diagram of our model. Our work shows that information scrambling plays a crucial role in understanding the dynamics of entanglement in an open quantum system and relates the entanglement phase transition to changes in quantum channel capacity.

DOI: 10.1103/PhysRevLett.125.030505

A generic unitary evolution of a quantum many-body system scrambles information. Any local degrees of freedom that are initially in an unentangled state become increasingly more entangled with the rest of the system, making the information encoded in them effectively unrecoverable [1–3]. The scrambling dynamics [4–7], evidenced by the growth of the entanglement entropy toward an extensive value [8–11], underlies the rich complexity of quantum dynamics and the fact that simulating it is beyond the capability of classical computers.

In a realistic system, however, unitary dynamics is often interspersed by occasional measurements of local observables made by external observers either controlled or accidental. This process disentangles the measured degrees of freedom from the rest of the system, which may reduce the entanglement entropy. Thus, it is natural to ask under what conditions the growth of entanglement is tamed to a point allowing efficient classical simulations of the quantum dynamics [12,13].

This question has been addressed in a number of recent works. In the special case of noninteracting fermions, quantum states with volume scaling entanglement (volume-law phase) are unstable to any small rate of measurements in local occupation basis, leading to steady states in which the entropy only scales with the boundary area of a region (area-law phase) [14]. However, the corresponding behavior in generic interacting systems appears to be much more subtle and has not been fully understood. On the one hand, Refs. [15–17] suggested that the interplay between the unitary dynamics and measurements can lead to a transition between two distinct phases: for sufficiently small measurement rates, the system remains stable in the volume-law phase, while it undergoes a transition into an area-law phase as the rate exceeds a certain critical value. On the other hand, in its early version, Ref. [17] pointed out that this phase transition cannot be explained by a simple competition between rates of entanglement growth and measurements, as it would always predict the area-law phase for nonzero measurement rates.

In this Letter, we show that a central ingredient for understanding the entanglement phase transition is the effective quantum error correction enabled by scrambling unitary dynamics. Using simple concepts from quantum information theory, we provide new insight on the mechanism that drives the phase transition. Naively, the phase transition seems to hinge on the competition between the rate of entanglement generation by unitary gates and that of disentanglement by measurements. If this perspective is true, the volume-law phase is unstable against an arbitrarily small rate of measurements since the competition is fundamentally not symmetric. Given a bipartition, a local unitary gate may change the entanglement only when it acts nontrivially across the boundary of two subsystems. In contrast, the effect of the measurements could be nonlocal: by disentangling all of the measured qubits inside a subsystem, the rate of entanglement reduction may be extensive. Thus, measurements would always overwhelm the entanglement generation and destabilize the volume-

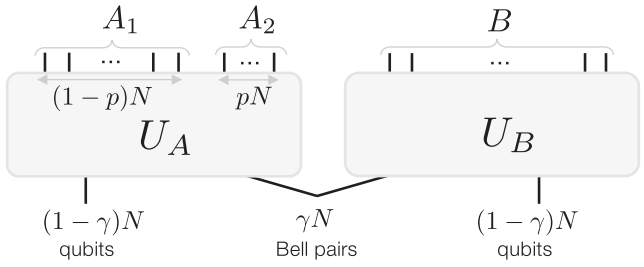

FIG. 1. Quantum state of $2N$ qubits generated by applying unitaries $U_{A(B)}$ to γN Bell pairs. Measuring p fraction of qubits (A_2) does not reduce the entanglement between $A = A_1A_2$ and B as long as $1 - p > \gamma$ in the limit $N \to \infty$.

law phase. Here, we argue that this is not the case when information scrambling is taken into account.

Our key observation is that nonlocal effects of sparse measurements are greatly suppressed due to the natural quantum error correction (QEC) property of scrambling dynamics. If quantum information is sufficiently scrambled by unitary evolution, correlations between two subsystems are hidden in highly nonlocal degrees of freedom and cannot be revealed by any local measurements. In such case, sparse local measurements, despite their extensive number, cannot decrease the entanglement entropy significantly. To illustrate this point and quantify the condition under which the entanglement is robustly protected against local measurements, we improve and apply the quantum decoupling theorem to a specially constructed toy model [18,19], showing the stability of the volume-law phase. We find that the mechanism of the protection is equivalent to that of the QEC scheme [18–20]. Motivated by this understanding, we introduce a new model and analyze its dynamics both analytically and numerically to obtain the phase diagram. Furthermore, we establish an exact relation between the steady-state entanglement entropy and the quantum channel capacity of quantum dynamics.

Protection against measurement.—We now illustrate how entanglement can be protected against measurements using a well-studied toy example from quantum information theory [19,21–23]. Consider a system of $2N$ qubits ($N \gg 1$) as shown in Fig. 1. Initially, the two halves of the system, A and B, share γN Bell pairs ($0 < \gamma < 1$), which control the amount of the entanglement between the two. The two subsystems are evolved independently with unitaries U_A and U_B, respectively. We assume U_A is a random unitary drawn from the Haar distribution (or any unitary 2-design), and U_B can be arbitrary. Following this evolution, a fraction p of the qubits in A is measured. The pertinent question is by how much these measurements reduce the entanglement between A and B. We shall show that under a certain condition the change of entanglement entropy due to the measurements vanishes in the thermodynamic limit even though an extensive number of qubits are being disentangled. Note that this result can be generalized to incorporate measurements performed on both A and B by sequentially analyzing the effect of measurements.

We first simplify the problem. Since U_B does not affect the entanglement, we may replace B with its minimal effective degrees of freedom $\tilde{B}$ entangled with A, i.e., the original γN entangled qubits. Also, we divide A into two parts: subsystem A_1 refers to the unmeasured qubits and subsystem A_2 contains the measured ones. We now apply the decoupling theorem [19,21–23] to this setup, which will imply that, for a sufficiently small measurement fraction p, the reduced density matrix of A_2 and $\tilde{B}$ approximately factorizes

$$\mathbb{E}_{U_A}[||\rho_{A_2\tilde{B}}(U_A) - \rho_{A_2}^{\max} \otimes \rho_{\tilde{B}}||_1] \leq 2^{-(1-2p-\gamma)N/2}. \quad (1)$$

Here, the left-hand side denotes the distance, in the L_1 norm, between the exact density matrix $\rho_{A_2\tilde{B}}$ and a factorized one where $\rho_{A_2}^{\max}$ is the maximally mixed state on the measured part A_2. $\mathbb{E}_U[\cdot]$ represents averaging over the random unitaries. The inequality implies that the measured qubits are effectively decoupled from $\tilde{B}$ for $N \gg 1$, provided that the number of unmeasured qubits A_1 is more than half of the total system $A\tilde{B}$, or equivalently

$$\gamma + p < \frac{1}{2}(1 + \gamma), \quad (2)$$

or simply $\gamma < 1–2p$. If this inequality is satisfied, then any observable in A_2 contains no information about $\tilde{B}$ and vice versa. Therefore, measuring one subsystem does not affect the other, up to an error exponentially small in N. In particular, any projection (due to measurements) acting on A_2 does not alter $\rho_{\tilde{B}}$, and the entanglement entropy of subsystem B is unchanged. In fact, one can show that even the initial γN Bell pairs can be reconstructed by local operations in A_1 with an exponentially good precision [20].

The inequality in Eq. (2) is enough to prove the stability of volume-law scaling of the entanglement entropy in the presence of extensive number of measurements. However, it is not tight. This is because in deriving the inequality we assumed that qubits in A_2 are discarded (i.e., qubit loss errors), whereas in our situation they are projectively measured, leaving their measurement outcomes as *accessible classical information*. In [24], we develop an improved decoupling equality, in which the measurement outcomes from A_2 are treated as accessible information. This leads to a tight bound

$$\gamma < 1 - p \quad (3)$$

in the limit $N \to \infty$. This inequality can be saturated by typical Haar random unitaries. An intuitive way to understand this new result is to realize that the measurement processes of pN qubits involve entangling those qubits

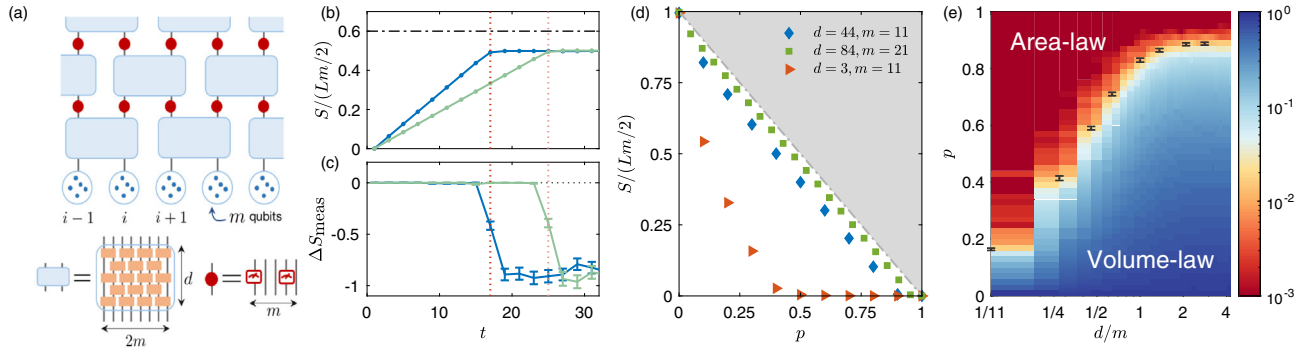

FIG. 2. (a) A model with tunable degrees of information scrambling d and measurements p. An array of m-qubit blocks undergoes layers of unitary gates (light blue) and random projective measurements (red). Each unitary acting on neighboring blocks comprises independently random 2-qubit gates (orange). Each measurement projects a randomly chosen p fraction of qubits in each block. (b),(c) Entanglement dynamics with $m = 11$, $d = 44$, and $p = 0.4$ for two different system sizes $L = 32$ (blue) and 48 (light green). (b) The growth of entanglement density as a function of time t. The dash-dotted line indicates the upper bound $1 - p$. (c) Change in the entanglement entropy before and after projective measurements at each time step. (d) Steady-state entanglement entropy per qubit as a function of p for $(d, m) = (44, 11)$, (84,21), and (3,11). (e) Phase diagram for $m = 11$. The color-coded background displays the half-chain entanglement entropies in steady states, normalized by the number of qubits $Lm/2 = 176$. Black markers indicate the phase transition points extracted from finite size scaling analysis up to $L = 64$. The numerical results in (b)–(e) are averaged over 240 different realizations of random circuits and measurements.

with an equal number of auxiliary qubits representing the environment (or classical measurement devices). These additional degrees of freedom effectively add to the right-hand side of Eq. (2), i.e., $\gamma + p < (1 + \gamma + p)/2$, leading to the tight bound.

So far, we have considered an ideal situation where the Bell pairs are hidden over the entire Hilbert space via a nonlocal unitary. However, we emphasize that such information scrambling is a generic property of quantum dynamics even in local systems [8–11,34]. In such cases, we expect that the amount of entanglement reduction is governed by the competition between the rate of effective information scrambling and that of projective measurements.

Model and phase diagram.—Having understood the mechanism to protect the entanglement against measurements through scrambling, we turn to study a local 1D model in which the rates of effective information scrambling and measurements can be tuned independently.

Our model consists of a chain of L blocks, each containing a fixed number, $m \gg 1$, of qubits, as illustrated in Fig. 2(a). In each time step t, the system is evolved by a network of random unitaries $U_d(i, t)$ acting on pairs of neighboring blocks at i and $i + 1$, supplemented by projective measurements. Crucially, the unitaries $U_d(i, t)$ are constructed from an internal network consisting of d layers of independent random 2-qubit gates (drawn from any unitary 2-design). Thus, the parameter d controls the degree of information scrambling within a single $U_d(i, t)$, which becomes maximally scrambling in the limit $d/m \gg 1$. In this limit the distribution of $U_d(i, t)$ approaches a unitary 2-design over $\mathrm{U}(2^{2m})$ [34]. After applications of the $U_d(i, t)$ on pairs of blocks, a fraction p of the qubits in each block is randomly chosen to be measured in the computational basis [35]. We note that the special case of our model, $d = 1$, is closely related to the previously studied ones [15–17].

Before obtaining a quantitative phase diagram from numerical simulations [Fig. 2(e)], one can already predict the stability of volume-law phase in the limit $m \gg 1$ and $d/m \gg 1$. Consider the unitary evolution $U_d(i, t)$ for a pair of blocks. If we identify the pair of blocks as subsystem A and the rest of the system as B, we can use the decoupling inequality as discussed above. As long as the average entropy per qubit γ satisfies the criteria in Eq. (3), the measured qubits contain almost no information about the rest of the system (up to corrections exponentially small in m). Here, the entanglement reduction is suppressed by information scrambling within the blocks. Over multiple time steps, quantum information becomes scrambled over a larger region, further protecting the entanglement from measurements. Thus we expect a stable volume-law phase in this regime.

We can also make a definitive statement about the other extreme of small d and high measurement rate. For example, consider $d = 1$, $m \gg 1$, and $p = 1 - 1/m$. In this case there is no room for scrambling; thus, the probability that a single qubit becomes entangled to other qubits at distance x away (in units of qubit blocks) is exponentially suppressed as $\sim(1/m)^{mx}$ because the information encoded in the qubit needs to propagate without being projected at least $\sim mx$ time steps. This implies area-law entanglement [14]. Therefore, we expect a phase transition between the two extreme cases.

We now complement the theoretical arguments with a numerical simulation of the half-chain entanglement

entropy $S(t)$ starting from the initial state $|\Psi_0\rangle = |0\rangle^{\otimes mL}$. We construct the unitary operators $U_d(i,t)$ from random 2-qubit Clifford gates drawn from a uniform distribution instead of taking Haar random unitaries. Such $U_d(i,t)$ still approaches a unitary 2-design as d increases [24]; hence, this simplification does not affect our predictions, while allowing scalable numerical simulation [36–39]. Furthermore, the wave function evolved under Clifford gates always exhibits a flat entanglement spectrum with respect to any bipartition. Thus, different measures of entanglement entropy, e.g., von Neumann versus Rényi entropies, yield the same value. In the following, we focus on $m = 11$.

We first consider a strongly scrambling regime, $d/(2m) \gtrsim 1$, where the unitary network within a single block effectively acts as a random $2^{2m} \times 2^{2m}$ unitary [24,34]. We test if the scrambling property of individual blocks leads to the robust volume-law entanglement of the entire system. Figures 2(b) and 2(c) show the detailed dynamics of the entanglement entropy for two different system sizes. Clearly, the entropy rescaled by the subsystem size exhibits a strict linear growth until it saturates to a constant value. The convergence of these values confirms the volume-law scaling of the entropy [24]. Moreover, we can directly compute how much the entanglement entropy changes, $\Delta S_{\text{meas}}(t)$, following projective measurements in each time step. Figure 2(c) confirms our prediction that in the strongly scrambling regime $d/(2m) \gtrsim 1$ and $m \gg 1$, the entanglement is unchanged by measurements until it reaches a saturation value set by the maximal entanglement that can be protected by the scrambling dynamics [40]. Once saturated, the entanglement added by the unitary gates pushes the entropy above the threshold of the decoupling theorem and it is reduced back to the saturation value by the subsequent measurements. Thus, upon reaching the saturation value, we see a jump of ΔS_{meas} from near zero to a negative value. We further note that the saturation value approaches its maximum, $1 - p$, as m is increased in this regime [Fig. 2(d)]. This is natural since our tight bound in Eq. (3) becomes exact when $m \to \infty$, and it predicts that each qubit on average contributes $\gamma = 1 - p$ to the global entanglement. We note that this analysis does not hold in the weakly scrambling regime $d/(2m) \lesssim 1$, e.g., $d = 3$, $m = 11$ [Fig. 2(d)].

We now turn to the phase transition that occurs when d is decreased or p is increased. From numerical simulations, we compute the half-chain entanglement per qubit and tripartite mutual information in the steady state for various L and p for a fixed d [24]. We perform a finite size scaling analysis in order to extract the critical measurement fraction p_c as well as the correlation length critical exponent ν [15,41]. By repeating the analysis for various values of d, we obtain a two-dimensional phase diagram shown in Fig. 2(e). We find that the fitted critical exponent ν has a universal value around 1.2 independent of d and m, suggesting the universality of the transition [24]. When $d = 1$ the extracted critical value $p_c \approx 0.16$ is consistent with previously reported results [16,42]. More importantly, we find that the volume-law entangled phase extends to a higher measurement fraction, as d increases to $\sim m$, and then saturates for $d/(2m) \gtrsim 1$.

Discussion.—The existence of the stable volume-law phase has a direct interpretation in terms of QEC for quantum communications [18], where the primary goal is to devise an encoding scheme to transfer the maximum amount of quantum information over a noisy or lossy channel. The maximum amount of coherent quantum information that can be transmitted through such a channel is called the quantum channel capacity $\mathcal{Q}$ [19,43]. Previously, one of the most important applications of the decoupling theorem had been to show that, by using a random unitary encoding, it is possible to asymptotically transfer $1 - 2p$ logical qubits per physical qubit over a lossy channel in which a fraction p of the physical qubits is lost [19]. In our settings, the projective measurements are distinguished from qubit loss errors since their measurement outcomes are available as classical information. This allows achieving a higher quantum channel capacity $1 - p$ that we prove using a new decoupling inequality [24].

The connection between the quantum channel capacity and the volume-law phase can be made more precise in two different settings. In the specific setting of our 1D model, we considered the capacity within a pair of neighboring qubit blocks. Here, the quantum information we wish to protect is quantified by the entanglement entropy between the qubit blocks and the rest of the system. The random unitary circuit is equivalent to repeated encoding of the information without explicit decoding. Since this encoding scheme can protect $\sim(1 - p)2m$ logical qubits in each pair of m-qubit blocks [24], we expect that our system should exhibit a stable volume-law scaling of entanglement supported by those logical qubits.

In a more general setting, we consider the entire system dynamics as a quantum channel and investigate its quantum channel capacity $\mathcal{Q}$. To this end, we take the input state to be entangled with an auxiliary reference such that its reduced density matrix is ρ_{in}. Then, we ask how much entanglement with the reference can be recovered from the combination of the output system density matrix ρ_{out} and a set of classical measurement outcomes after a long time evolution. This can be quantified by the *coherent information* $\mathcal{I}_c(\mathcal{N}, \rho_{\text{in}})$ [44]. For a quantum channel $\mathcal{N}$ consisting of unitary evolution interspersed with measurements (in any positive-operator valued measures), we show that [24]

$$\mathcal{Q} = \max_{\rho_{\text{in}}} \mathcal{I}_c(\mathcal{N}, \rho_{\text{in}}) = \max_{\rho_{\text{in}}} \langle S(\rho_{\text{out}}) \rangle \tag{4}$$

where $\langle S(\rho_{\text{out}}) \rangle$ is the von Neumann entropy of ρ_{out}, averaged over all possible measurement outcomes during

the time evolution. We note that the first equality in Eq. (4) is not generically valid, but it holds for a class of so-called *degradable* quantum channels that include our cases [19,43,44]. Using the second equality, we establish an exact connection between quantum channel capacity and the average entropy of a system undergoing any unitary evolution interspersed by measurements. A similar connection was first suggested in a recent paper by Gullans and Huse [41].

In Ref. [41], $\langle S(\rho_{\text{out}})\rangle$ for the maximally mixed initial state was shown to undergo a phase transition, which coincides with the entanglement phase transition for pure initial states. Specifically, in the volume-law phase, $\langle S(\rho_{\text{out}})\rangle$ remains extensive at late time, while in the area-law phase, it rapidly approaches a value of order one. This transition was dubbed the purification phase transition [41]. The equivalence between the purification and entanglement phase transitions has later been established analytically for local Haar random unitary circuits with measurements [45]. Therefore, Eq. (4) also builds a quantitative connection between the quantum channel capacity and the entanglement phase transition. We note that, in random circuit models studied in Refs. [15,16,41,45,46], the channel $\mathcal{N}$ itself is random, whose average $\mathcal{I}_c$ is maximized for the maximally mixed input, furthering the connection [24].

We note that, after we conjectured the relation between the quantum channel capacity and entanglement phase transition in the earlier preprint version of this paper, Ref. [41] provided the first quantitative evidence, proving that the single-shot quantum channel capacity is upper bounded by the average entropy of the output and showed that the stabilizer circuit saturates the bound. In this new version, we further prove a generic equality between output entropy and quantum channel capacity by considering the classical information in measurement outcomes as part of the channel.

We thank M. Gullans, D. Huse, X. Chen, Y. Li, I. Kim, A. Nahum, and Q. Zhuang for useful discussions. S. C. acknowledges support from the Miller Institute for Basic Research in Science. Y. B. acknowledges support from the GSI program at UC Berkeley. X. L. Q. and E. A. are supported in part by the Department of Energy Project No. DE-SC0019380. E. A. acknowledges support from the ERC synergy grant UQUAM and from the Gyorgy Chair in Physics at UC Berkeley.

S. C. and Y. B. contributed equally to this work.

[1] J. M. Deutsch, Phys. Rev. A **43**, 2046 (1991).
[2] M. Srednicki, Phys. Rev. E **50**, 888 (1994).
[3] M. Rigol, V. Dunjko, and M. Olshanii, Nature (London) **452**, 854 (2008).
[4] P. Hayden and J. Preskill, J. High Energy Phys. 09 (2007) 120.
[5] Y. Sekino and L. Susskind, J. High Energy Phys. 10 (2008) 065.
[6] S. H. Shenker and D. Stanford, J. High Energy Phys. 03 (2014) 067.
[7] P. Hosur, X.-L. Qi, D. A. Roberts, and B. Yoshida, J. High Energy Phys. 02 (2016) 004.
[8] A. Nahum, J. Ruhman, S. Vijay, and J. Haah, Phys. Rev. X **7**, 031016 (2017).
[9] C. W. von Keyserlingk, T. Rakovszky, F. Pollmann, and S. L. Sondhi, Phys. Rev. X **8**, 021013 (2018).
[10] A. Nahum, S. Vijay, and J. Haah, Phys. Rev. X **8**, 021014 (2018).
[11] C. Jonay, D. A. Huse, and A. Nahum,arXiv:1803.00089.
[12] D. Aharonov, Phys. Rev. A **62**, 062311 (2000).
[13] G. Vidal, Phys. Rev. Lett. **93**, 040502 (2004).
[14] X. Cao, A. Tilloy, and A. De Luca, SciPost Phys. **7**, 024 (2019).
[15] B. Skinner, J. Ruhman, and A. Nahum, Phys. Rev. X **9**, 031009 (2019).
[16] Y. Li, X. Chen, and M. P. A. Fisher, Phys. Rev. B **98**, 205136 (2018).
[17] A. Chan, R. M. Nandkishore, M. Pretko, and G. Smith, Phys. Rev. B **99**, 224307 (2019).
[18] M. A. Nielsen and I. L. Chuang, *Quantum Computation and Quantum Information* (Cambridge University Press, Cambridge, England, 2000).
[19] J. Preskill, Lecture notes for physics 219: Quantum computation, 2018.
[20] B. Schumacher and M. D. Westmoreland, Quantum Inf. Process. **1**, 5 (2002).
[21] I. Devetak, IEEE Trans. Inf. Theory **51**, 44 (2005).
[22] M. Horodecki, J. Oppenheim, and A. Winter, Commun. Math. Phys. **269**, 107 (2007).
[23] A. Abeyesinghe, I. Devetak, P. Hayden, and A. Winter, Proc. R. Soc. A **465**, 2537 (2009).
[24] See Supplemental Material at http://link.aps.org/supplemental/10.1103/PhysRevLett.125.030505 for the detailed information on numerical simulations, the finite-size scaling analysis, the relation between the quantum channel capacity and the entanglement phase transition, and the derivation of the improved decoupling inequality, which includes Refs. [25–33].
[25] D. P. DiVincenzo, D. W. Leung, and B. M. Terhal, IEEE Trans. Inf. Theory **48**, 580 (2002).
[26] D. A. Roberts and B. Yoshida, J. High Energy Phys. 04 (2017) 121.
[27] C. H. Bennett, D. P. DiVincenzo, J. A. Smolin, and W. K. Wootters, Phys. Rev. A **54**, 3824 (1996).
[28] A. R. Calderbank, E. M. Rains, P. W. Shor, and N. J. A. Sloane, Phys. Rev. Lett. **78**, 405 (1997).
[29] D. Gottesman, Phys. Rev. A **54**, 1862 (1996).
[30] Z. Webb, arXiv:1510.02769.
[31] J. Houdayer and A. K. Hartmann, Phys. Rev. B **70**, 014418 (2004).
[32] N. Kawashima and N. Ito, J. Phys. Soc. Jpn. **62**, 435 (1993).
[33] B. Collins, Int. Math. Res. Not. **2003**, 953 (2003).

[34] F. G. S. L. Brandão, A. W. Harrow, and M. Horodecki, Commun. Math. Phys. **346**, 397 (2016).
[35] For noninteger pm, the number of measured qubits is determined from a binomial distribution between $\lfloor pm \rfloor$ and $\lceil pm \rceil$ with mean pm.
[36] D. Gottesman, arXiv:quant-ph/9807006.
[37] S. Aaronson and D. Gottesman, Phys. Rev. A **70**, 052328 (2004).
[38] A. Hamma, R. Ionicioiu, and P. Zanardi, Phys. Lett. A **337**, 22 (2005).
[39] A. Hamma, R. Ionicioiu, and P. Zanardi, Phys. Rev. A **71**, 022315 (2005).
[40] We note that, for this purpose, we have only considered odd time steps since in even time steps projective measurements destroy local entanglement within the qubit blocks that are generated by immediately preceding $U_d(i,t)$.
[41] M. J. Gullans and D. A. Huse, arXiv:1905.05195.
[42] Y. Li, X. Chen, and M. P. A. Fisher, Phys. Rev. B **100**, 134306 (2019).
[43] M. M. Wilde, *Quantum Information Theory* (Cambridge University Press, Cambridge, England, 2013).
[44] I. Devetak and P. W. Shor, Commun. Math. Phys. **256**, 287 (2005).
[45] Y. Bao, S. Choi, and E. Altman, Phys. Rev. B **101**, 104301 (2020).
[46] C.-M. Jian, Y.-Z. You, R. Vasseur, and A. W. W. Ludwig, Phys. Rev. B **101**, 104302 (2020).